JOURNAL OF VIROLOGY, Sept. 2004, p. 8960–8970 Vol. 78, No. 17
0022-538X/04/$08.00+0 DOI: 10.1128/JVI.78.17.8960–8970.2004

Replication and Cytopathic Effect of Oncolytic Vesicular Stomatitis Virus in Hypoxic Tumor Cells In Vitro and In Vivo

John H. Connor,[1]* Christine Naczki,[2] Costas Koumenis,[2] and Douglas S. Lyles[1]

Department of Biochemistry[1] and Department of Radiation Oncology,[2] Wake Forest University School of Medicine, Winston-Salem, North Carolina

Received 26 November 2003/Accepted 15 April 2004

Tumor hypoxia presents an obstacle to the effectiveness of most antitumor therapies, including treatment with oncolytic viruses. In particular, an oncolytic virus must be resistant to the inhibition of DNA, RNA, and protein synthesis that occurs during hypoxic stress. Here we show that vesicular stomatitis virus (VSV), an oncolytic RNA virus, is capable of replication under hypoxic conditions. In cells undergoing hypoxic stress, VSV infection produced larger amounts of mRNA than under normoxic conditions. However, translation of these mRNAs was reduced at earlier times postinfection in hypoxia-adapted cells than in normoxic cells. At later times postinfection, VSV overcame a hypoxia-associated increase in α subunit of eukaryotic initiation factor 2 (eIF-2α) phosphorylation and initial suppression of viral protein synthesis in hypoxic cells to produce large amounts of viral protein. VSV infection caused the dephosphorylation of the translation initiation factor eIF-4E and inhibited host translation similarly under both normoxic and hypoxic conditions. VSV produced progeny virus to similar levels in hypoxic and normoxic cells and showed the ability to expand from an initial infection of 1% of hypoxic cells to spread through an entire population. In all cases, virus infection induced classical cytopathic effects and apoptotic cell death. When VSV was used to treat tumors established in nude mice, we found VSV replication in hypoxic areas of these tumors. This occurred whether the virus was administered intratumorally or intravenously. These results show for the first time that VSV has an inherent capacity for infecting and killing hypoxic cancer cells. This ability could represent a critical advantage over existing therapies in treating established tumors.

Solid tumors are seldom homogeneous, but instead, they have different microenvironments that can profoundly influence therapeutic approaches. Perhaps the best-studied component of the tumor microenvironment is the presence of low oxygen tension, or hypoxia. Hypoxic areas within the tumor mass provide significant difficulties for standard anticancer therapy, as these areas present a physical barrier to chemotherapeutic agents and are more resistant to radiation therapy because of the lack of ionizable oxygen (10, 17, 23). Hypoxic stress can also select for the survival of cancer cells that are deficient in p53 function (16), leading to the expansion of cells that are more resistant to conventional cancer therapies. Furthermore, tumor hypoxia correlates with an overall poor patient prognosis (23). These complications have led to a number of efforts to define new modalities that are capable of killing hypoxic cancer cells (17).

Using viruses as oncolytic agents has recently emerged as a viable and useful antitumor strategy (7, 18). Oncolytic viruses have the ability to directly kill cancer cells and the potential to stimulate the production of cytokines with anticancer activity. Further, the ability to genetically alter virus vectors provides the opportunity to tailor these viruses to specific aspects of tumor development or tumor biology. A variety of different viruses have been tested as oncolytic agents, including DNA viruses such as adenovirus (13) and herpes simplex virus (2) and RNA viruses such as Newcastle disease virus (35), reovirus (20), influenza virus (8), and vesicular stomatitis virus (VSV) (6, 36). One or more of these agents may have the potential for treating tumors with extensive hypoxic areas that are resistant to other therapies. The experiments presented here tested this hypothesis with VSV.

Previous studies have shown that VSV can infect and kill a diverse set of cancer cells (6, 36). The advantages of this virus are that oncolytic strains do not appear to be pathogenic in humans, replicate entirely in the cytoplasm, and have no known transforming abilities. VSV was shown to infect and kill cancer cells while sparing nontransformed cells in tissue culture because of defects in antiviral responses in the tumor cells (6, 36, 37). This oncolytic behavior has also been shown in vivo, where VSV injection affected the growth of tumors in both xenograft (5, 36) and syngeneic tumor models (14, 15, 24, 28, 37) following intratumoral or systemic administration.

While these studies have elegantly demonstrated that, in vitro, VSV's ability to kill cancer cells depends on these cells being defective in their antiviral response, they have not addressed whether this property is the sole determinant in the success of VSV in treating established tumors in vivo. VSV's tumoricidal properties may be attributable to several advantages as an antitumor agent, especially if it is able to overcome physiological barriers in established tumors, such as hypoxic microenvironments.

On the cellular level, hypoxia induces several adaptive stress responses, including an inhibition of DNA synthesis (31), RNA synthesis, and a general inhibition of protein translation (22, 27). At the same time, hypoxia selectively promotes the transcription and translation of hypoxia-adaptive genes such as vascular endothelial growth factor and hypoxia-inducible fac-

* Corresponding author. Present address: Wake Forest University School of Medicine, Department of Microbiology and Immunology, Medical Center Blvd., Winston-Salem, NC 27157. Phone: (336) 716-2270. Fax: (336) 716-9928. E-mail: jconnor@wfubmc.edu.

tor 1 (HIF1) (10). These cellular changes have been seen by many as an opportunity to directly target tumor therapy to take advantage of these intracellular changes, ranging from drugs that concentrate in hypoxic tissue (11) to toxic gene expression that is driven by promoters that are activated under hypoxia (9, 30).

Our previous studies led us to hypothesize that VSV infection resulted in a cellular stress response and that VSV has adapted to translate protein during this stress response. Because VSV and hypoxia both result in an inhibition of host protein synthesis (12, 27), we hypothesized that hypoxic cells and VSV-infected cells translate proteins under similar circumstances (3, 12). We reasoned that VSV replication may be able to adapt to cells under hypoxic stress. In addition, because VSV is an RNA virus that produces its own RNA polymerase, it should not be sensitive to the hypoxia-induced inhibition of DNA and RNA synthesis in the way that DNA viruses are (33, 34). Our results indicate that there was an early effect of hypoxia that inhibited the translation of viral proteins, but the virus appeared to adapt to the hypoxic environment and overcome this inhibition as the infection progressed. VSV caused cytopathic effects (CPE) in hypoxic cells in tissue culture and spread under hypoxic conditions both in culture and in a tumor xenograft model. These data demonstrate that VSV has an inherent ability to replicate in hypoxic cells inside a tumor environment, which may be an additional advantage of using this virus to treat established tumors.

MATERIALS AND METHODS

Chemicals, unless otherwise stated, were purchased from Fisher Scientific. Okadaic acid and microcystin were purchased from Alexis Pharmaceuticals. EF-5 and the anti-EF-5 antibody were supplied by the University of Pennsylvania (Sidney Evans). Rabbit anti-VSV glycoprotein G (anti-VSV-G) was purchased from Research Diagnostics, Inc. Phospho- and total α subunit of eukaryotic initiation factor 2 (eIF-2α) and eIF-4E antibodies were purchased from Signal Transduction Labs. Anti-HIF1α was purchased from Becton Dickenson, and anti-actin was purchased from Santa Cruz. Anti-poly(ADP-ribose) polymerase (anti-PARP) was from Roche Biochemicals. Fluorescein isothiocyanate (FITC)-conjugated anti-rabbit antibody was purchased from Molecular Probes.

Virus infections. HeLa cells were cultured in Dulbecco's modified Eagle medium (DMEM; Gibco-BRL) containing 10% fetal bovine serum (FBS) and 2 mM glutamine. Cells were grown to 80 to 90% confluence and were infected with wild-type VSV (Indiana serotype, Orsay strain) in DMEM with 10% FBS at a multiplicity of infection (MOI) of 10 or 0.01 PFU/cell in a small volume (2.5 ml in a 60-mm-diameter dish, 500 μl for a six-well dish). At 1 h postinfection (hpi), the culture volume was doubled by the addition of DMEM plus 10% FBS.

Establishment of hypoxia in vitro. Cells were subjected to hypoxia by incubation in a hypoxia chamber (Sheldon Labs) under conditions of 90% N_2, 5% CO_2, and 5% H_2. Cells were cultured in a minimal volume of media (2.5 ml for a 60-mm-diameter dish). Cell dishes were swirled to promote the exchange of gas from the media following introduction to the chamber. One set of cells (labeled "hypoxia") was immediately infected with VSV. A second set of cells (labeled "hypoxia adapted") was infected 2 h after the cells had adapted to the hypoxic conditions. Hypoxic conditions were maintained in the chamber through the use of an active palladium catalyst which converted O_2 and H_2 to water, effectively removing any trace O_2 contamination introduced by entry and exit from the hypoxia chamber.

Immunoblotting. Infected or mock-infected cells were lysed in a 60-mm-diameter dish by using 1 ml of EBC buffer containing 1 mM phenylmethylethyl fluoride, 1 mM benzamidine, 100 nM okadaic acid, and 100 nM microcystin (12). Lysates were spun at 10,000 × *g* for 8 min in a refrigerated centrifuge, and 360 μl of the supernatant was added to 40 μl of 10× sample buffer for sodium dodecyl sulfate-polyacrylamide gel electrophoresis (SDS-PAGE). Equal volumes of lysates corresponding to approximately 30 μg of total protein were electrophoresed on SDS–12% PAGE gels for M protein, eIF-2α, eIF-4E, and actin blots and on 6% gels for HIF1α blots. Following electrophoresis, gels were electroblotted onto nitrocellulose and blocked in Tris-buffered saline (pH 7.5) plus 5% dry milk. Antibodies were diluted as recommended by the manufacturers. Band intensities were quantitated by first scanning the film and then analyzing the images with Quantity One software (Bio-Rad).

Metabolic labeling and determination of rate of protein synthesis. HeLa cells were mock infected or infected with VSV and then labeled with [^{35}S]methionine for 10 min at various times postinfection, as described previously (12). Following labeling, cells were washed three times with phosphate-buffered saline and lysed in 400 μl of radioimmunoprecipitation assay buffer for 10 min at 4°C. Lysates were spun at 10,000 × *g* for 8 min. Three hundred sixty microliters of supernatant was added to 40 μl of 10× SDS-PAGE sample buffer, and 10 μl was electrophoresed on an SDS–12% PAGE gel. Gels were stained with Coomassie blue to check for even protein loading, and then these gels were analyzed by phosphorescence imaging (Molecular Dynamics, Inc.). The quantitation of phosphorescence intensities was analyzed with ImageQuant software. The rate of viral protein synthesis was determined from experiments by quantitation of the radioactivity in the viral L, G, N/P, and M bands in each lane. The rate of host protein synthesis was determined by quantitation of the radioactivity between the L and G bands, the N/P and M bands, and below the M band. Experiments were performed in triplicate, and average values along with standard deviation values are reported for each condition.

Phase-contrast and fluorescence microscopy. Phase-contrast images were taken by using an Olympus IX70 microscope, an RT color charge-coupled device camera (Diagnostic Instruments), and the SPOT analysis image acquisition software. Epifluorescence images were taken by using a Nikon Eclipse TE300 with Plan Fluor objectives, a Retiga EX imaging camera, and the Q-capture software package (Quantitative Imaging Corp.). Images were taken with different filter sets and were recombined in Adobe Photoshop to create overlay images.

Tumor growth and staining. For intratumoral injections, nude mice were flank injected with 2×10^6 C6 glioblastoma cells in 100 μl of phosphate-buffered saline. When tumors were between 500 and 1,000 mm^3, they were injected intratumorally with 10^7 PFU of VSV. Animals were kept in a sterile barrier facility for 23 h and then injected intraperitoneally with 300 μl of EF-5 dye. One hour after EF-5 injection, mice were euthanized (CO_2) and the tumor was dissected from the flank and frozen. For intravenous injections, nude mice were flank injected with 2×10^6 mouse embryonic fibroblasts (MEFs) transformed with the oncogenic Ras gene (27). When tumors were between 400 and 500 mm^3, mice were tail vein injected with 5×10^7 PFU of VSV. The animals were kept in a sterile barrier facility for 36 h, then injected intraperitoneally with 300 μl of EF-5 dye, and treated as described for intratumoral injections. In all cases, tumors were then embedded in tissue freezing medium and sectioned at 7 μm in a cryotome. Sections were fixed in cold 95% ethyl alcohol. Following rehydration, cells were further fixed in 100% methanol for 5 min and blocked in 3% bovine serum albumin. EF-5 was detected with anti-EF-5 (University of Pennsylvania), and VSV replication was detected with an antibody against VSV-G followed by secondary anti-rabbit antibody conjugated to FITC.

Northern blotting. Blotting was performed as described earlier (12). Briefly, infected or mock-infected cells were lysed in 60-mm-diameter dishes by using the total RNA isolation kit (Promega), and RNA was purified as per the manufacturer's instructions. Five micrograms of total RNA from each sample was glyoxylated and separated on a 1% agarose gel. Following acridine orange staining, to check for loading, RNA was transferred onto nitrocellulose (Genescreen Plus; NEN) and probed with an M gene cDNA probe. The results were determined by phosphorescence imaging and analyzed with ImageQuant software.

RESULTS

It is well established that hypoxic stress causes an inhibition of cellular RNA and protein synthesis. Recent evidence suggests that this is due to the activation of cellular control mechanisms and not the depletion of biosynthetic precursors (22). We tested whether these cellular inhibition mechanisms would impair the cytoplasmically replicating oncolytic virus VSV. To determine whether VSV could productively infect hypoxic cancer cells, we used HeLa cells as a model. HeLa cells are derived from cervical carcinoma, a neoplasm known to develop areas of severe hypoxia (23). Consistent with this, HeLa cells can survive for relatively long periods of time (>48 h) under extremely hypoxic-anoxic conditions. Cells were infected under single-cycle growth conditions (an MOI of 10 PFU/cell) in a

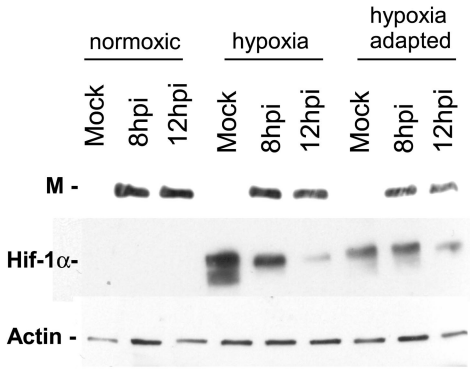

FIG. 1. Expression of VSV protein in HeLa cells following infection under normoxic or hypoxic conditions. Extracts from mock- and VSV-infected cells were analyzed by Western blotting (see Materials and Methods) with antibodies against the VSV M protein, the hypoxia-induced protein HIF1α, and actin. Blots are representative of the results from three separate experiments.

normoxic environment and also either immediately or 2 h after being placed in the hypoxic environment. The latter condition was intended to allow time for the hypoxic response to develop. Cells infected under these conditions are referred to as hypoxic and hypoxia-adapted, respectively. The status of viral gene expression was tested at 8 and 12 hpi. The 8-hpi time point represents a time of maximal viral protein synthesis and mRNA accumulation under normal conditions, whereas by 12 hpi, both viral mRNA and viral protein synthesis are markedly inhibited during a normal infection (1).

We first determined by immunoblotting whether viral protein accumulated during infection of hypoxic cells. As shown in Fig. 1, VSV matrix (M) protein was present in control normoxic infected cell lysates at both 8 and 12 hpi and was also present in hypoxic and hypoxia-adapted cells infected with VSV. Levels of M protein appeared to be similar in normoxic and hypoxic infected cells, but there was a lower level of protein accumulation in cells under hypoxia-adapted conditions at both time points. These lysates were also probed for the accumulation of HIF1α as a control for the induction of a cellular response to hypoxia. HIF1α was not present in normoxic cells but was significantly induced in the hypoxic, mock-infected cells, demonstrating that a hypoxic stress response was induced under our hypoxic conditions. Hypoxic and hypoxia-adapted cells that were infected with VSV showed some accumulation of HIF1α, but this induction was noticeably lower than that seen in mock-infected cells. This was likely due to viral suppression of host gene expression (1). Actin levels were also measured as a control for sample loading.

Hypoxia does not inhibit viral mRNA accumulation. The results shown in Fig. 1 demonstrate that VSV produced viral protein in a hypoxic environment, but in the hypoxia-adapted cells, there was less protein accumulation. This suggested that VSV was sensitive to the adaptation to hypoxia but raised the question of whether the inhibitory effect was at the level of mRNA production or the level of protein synthesis. Analysis of the accumulation of mRNA for the VSV M protein by Northern blots showed that, in normoxic cells, M mRNA had accumulated by 8 hpi, but by 12 hpi, this level had decreased (Fig. 2A). This pattern was also observed in cells that were infected with VSV immediately after being placed in the hypoxia chamber (Fig. 2, hypoxia lanes), showing that viral mRNA accumulation was unaffected by the switch to an anoxic environment

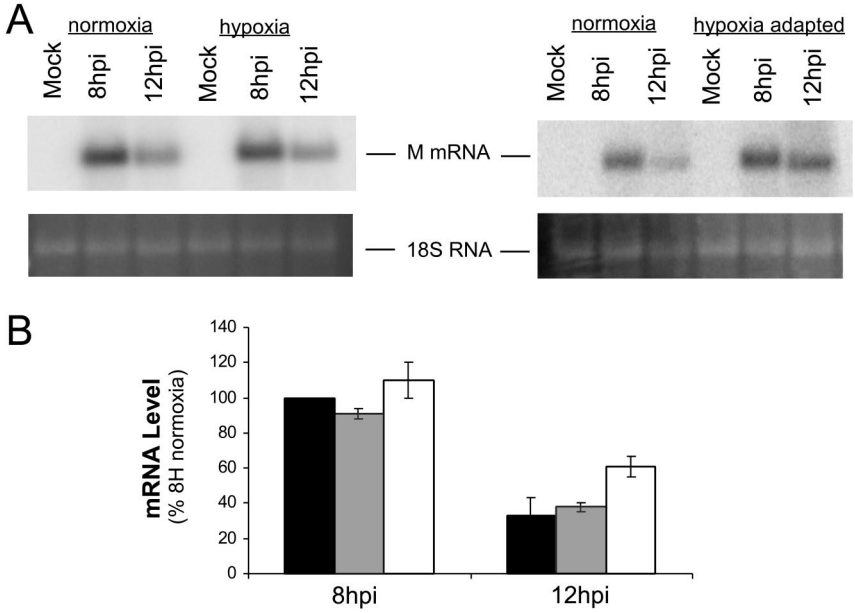

FIG. 2. Viral mRNA accumulation during infection of hypoxic cells. (A) Total RNA was prepared from HeLa cells mock infected (M) or infected with VSV for 8 and 12 hpi. RNA was separated on a 1% gel and transferred to nitrocellulose, and viral mRNA was detected by using a ^{32}P-labeled probe for M mRNA. Phosphorescence images of representative gels comparing infected normoxic and hypoxic cells (left) or normoxic and hypoxia-adapted cells (right) are shown at the top, with an acridine orange stain showing 18S RNA at the bottom. (B) Quantification of accumulation of M mRNA. Black bars, normoxic infection; gray bars, hypoxic infection; white bars, hypoxia-adapted infection. Values are normalized to normoxic infection at 8 hpi (8H). Values are means ± standard deviations of the results from three separate experiments.

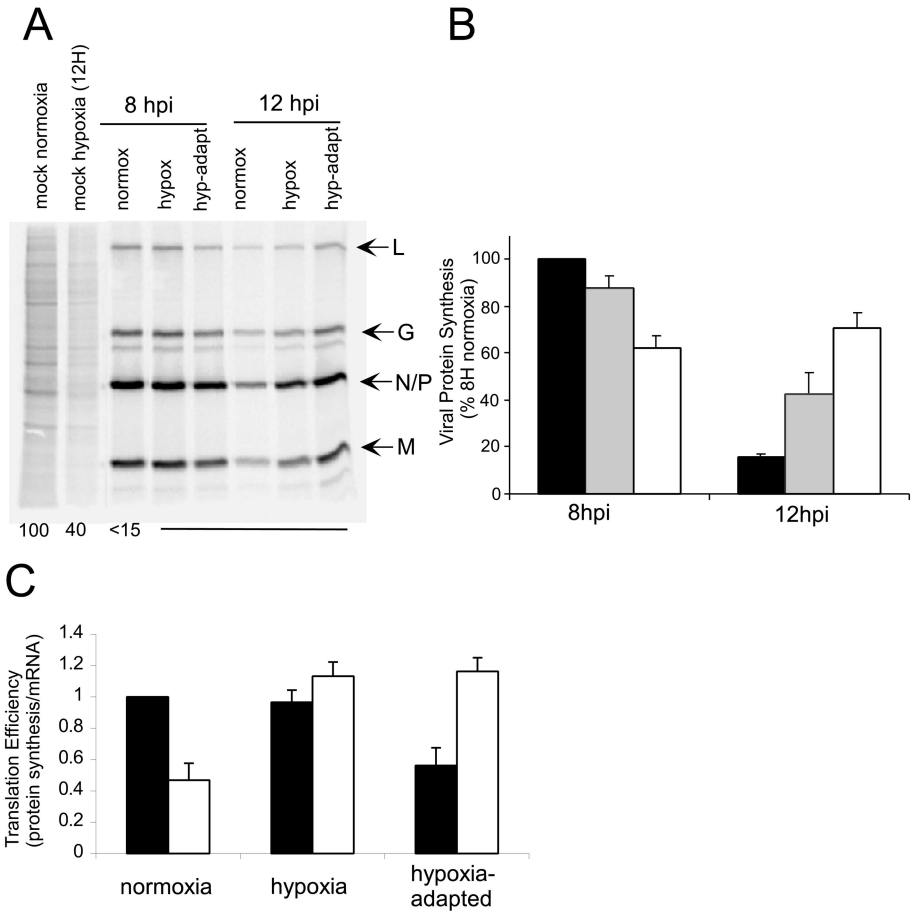

FIG. 3. Host and viral protein synthesis during hypoxia. (A) Cells were mock infected or infected with VSV in normoxic (normox), hypoxic (hypox), or hypoxia-adapted (hyp-adapt) conditions and labeled with [^{35}S]methionine for 10 min. Cell lysates were electrophoresed on an SDS–12% PAGE gel, a phosphorescence image of which is shown. Viral proteins are indicated to the right of the image, and a quantification of host protein synthesis is shown at the bottom of the gel. Bottom numbers show the average host protein synthesis values determined from signal strength in the entire lane, excluding viral proteins. (B) Quantification of viral protein synthesis. The rates of protein synthesis were determined from images similar to those shown in panel A as detailed in Materials and Methods for normoxic infection (black bars), hypoxic infection (gray bars), and hypoxia-adapted infection (white bars). (C) Translation efficiency of viral messages. The ratios of M protein synthesis to M mRNA (Fig. 2) at 8 hpi (black bars) and 12 hpi (white bars) are graphed. Values are normalized to the 8-hpi normoxia infection value.

coincident with infection. In the hypoxia-adapted cells there was a different pattern of viral mRNA expression. At 8 hpi, there was an increased accumulation of M mRNA in the hypoxia-adapted cells compared to the normoxic control, and the characteristic decrease in mRNA that was seen by 12 hpi in normoxic cells was not as dramatic (Fig. 2A). A quantitative analysis of multiple Northern blots is shown in Fig. 2B, where all values are normalized to the normoxic infection control at 8 hpi. At 8 hpi, there was a 15% increase in M mRNA in the infected hypoxia-adapted cells. At 12 hpi, mRNA levels in normoxic and hypoxic cells were only 30% of the 8-hpi value; in the hypoxia-adapted cells, the levels were twice as high, 60% of the 8-hpi control. These data indicate that VSV RNA synthesis was not markedly inhibited by hypoxia, and mRNA levels were actually increased by hypoxic stress.

VSV protein translation in hypoxic cells. Having established that VSV protein accumulation was decreased and viral mRNA was increased in hypoxia-adapted cells, we investigated whether there were changes in viral translation in cells undergoing hypoxic stress. Mock-infected or VSV-infected normoxic, hypoxic, and hypoxia-adapted cells were pulse-labeled with [^{35}S]methionine at 8 or 12 hpi and then analyzed by SDS-PAGE and phosphorimaging (Fig. 3A, left). The first two lanes show mock-infected normoxic and hypoxic cells. Cellular proteins are apparent as a gray smear in the lane, marked by some prominent bands. Mock-infected hypoxic cells showed an inhibition of protein synthesis at 12 h to approximately 40% of normoxic control levels. This decrease reflects the general inhibition of host protein synthesis seen during a hypoxic stress response (22, 27). In normoxic cells, VSV infection resulted in the shutoff of host protein synthesis by 8 hpi and the robust protein synthesis of the 5 viral proteins, L, G, N, P, and M, which can be seen as four bands in the infected-cell lanes. Similar results were seen when hypoxic and hypoxia-adapted cells were infected, but the rate of synthesis of viral proteins was diminished in the hypoxia-adapted cells. At 12 hpi, viral protein synthesis was dramatically inhibited in normoxic cells, consistent with earlier reports, but protein synthesis was not as dramatically inhibited in the hypoxic cells and even appeared to increase in hypoxia-adapted cells.

Figure 3B shows a quantification of these results. At 8 hpi, viral protein synthesis in hypoxia-adapted cells was 60% of the control. At 12 hpi, viral protein synthesis was only 15% of that at 8 hpi in the normoxic control. In hypoxic cells, viral protein synthesis only decreased to 40% of the control. Similarly, in hypoxia-adapted cells, translation at 12 hpi was not strongly decreased and, in fact, was slightly increased (to 70% of the normoxic control 8-hpi value). Examination of longer time points out to 16 hpi (data not shown) indicated that viral protein synthesis in hypoxia-adapted cells never reached the levels seen at 8 hpi in normoxic cells. Instead, viral protein synthesis in the hypoxia-adapted cells continued for a longer period of time. These results suggest that (i) adaptation to hypoxic stress has the ability to decrease viral protein synthesis at early times and (ii) at late times postinfection, there is less inhibition of viral protein synthesis in hypoxic cells.

These conclusions were supported by comparing the rate of protein synthesis to the amount of mRNA present under the different conditions to determine the extent to which the changes in viral protein synthesis were due to changes in mRNA levels. Figure 3C shows the ratio of the protein synthesis value from Fig. 3B divided by the mRNA level from Fig. 2B and will be referred to as the translation efficiency. Cells infected under normoxic conditions had reduced the translation efficiency of VSV mRNA approximately 50% at 12 hpi compared to 8 hpi. This inhibition was not seen during infection of hypoxic cells, where the translation efficiency remained unchanged. While translation decreased in these cells, this can be accounted for by the decrease in mRNA present (Fig. 2). In the hypoxia-adapted cells, translation of VSV mRNA was inhibited slightly at 8 hpi, but this inhibition appeared to be relieved by 12 hpi, when the translation efficiency reached a value of approximately 1.2, the same level seen in hypoxic cells that were infected with VSV.

Modification of translation initiation factors during VSV infection of hypoxic cells. Hypoxic stress induces the phosphorylation of eIF-2α through activation of the PERK kinase (27). Phosphorylation of eIF-2α by the double-stranded-RNA-activated kinase protein kinase R is also thought to inhibit translation of VSV mRNAs (4; J. H. Connor and D. S. Lyles, unpublished data). We therefore hypothesized that the eIF-2α phosphorylation may account for the inhibition of viral translation at early times postinfection in hypoxia-adapted cells. The phosphorylation state of eIF-2α under normoxic and hypoxic conditions was determined by Western blotting with phosphospecific antibodies against eIF-2α (Fig. 4A). There were distinct differences between normoxic and hypoxic infection conditions. Under normoxic conditions, there was very little phosphorylation of eIF-2α in mock-infected cells, but virus infection stimulated significant phosphorylation of eIF-2α by 8 hpi, which was maintained at 12 hpi. This phosphorylation is likely due to the activation of protein kinase R. Under hypoxic conditions, eIF-2α phosphorylation was increased at 2 h in mock-infected cells, the time at which VSV was added. Similar levels of eIF-2α phosphorylation were seen at 4 h in mock-infected cells. This is consistent with earlier reports (27) and shows that one difference between VSV infection of normoxic cells and hypoxia-adapted cells is that there is preexisting phosphorylated eIF-2α in the hypoxia-adapted cells. This result supports the idea that the lower levels of viral protein synthesis in hypoxia-adapted cells is due in part to preexisting eIF-2α phosphorylation.

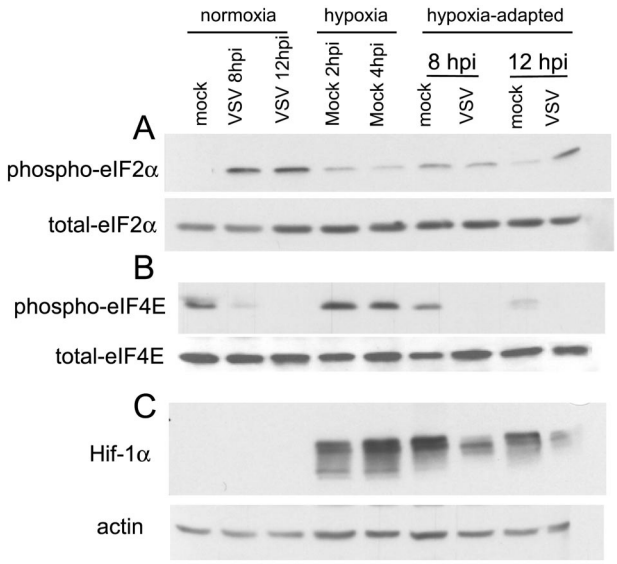

FIG. 4. eIF-2α and eIF-4E phosphorylation during VSV infection under normoxic or hypoxic conditions. Extracts from mock- and VSV-infected cells were analyzed by Western blotting (see Materials and Methods) with antibodies against total and phospho-eIF-2α (Ser51) (A), total and phospho-eIF-4E (Ser209) (B), and the hypoxia-induced protein HIF1α and actin (C). Blots are representative of the results from two separate experiments.

In hypoxia-adapted cells, both mock-infected and virus-infected cells showed an increase in phosphorylation at 8 hpi but not to the levels seen in VSV-infected normoxic cells. Thus, the reduced translational efficiency of viral mRNA in hypoxia-adapted cells at 8 hpi (Fig. 3C) cannot be accounted for by a higher level of eIF-2α phosphorylation. At 12 hpi, there was an additional increase in eIF-2α phosphorylation in the hypoxia-adapted cells that were infected with virus but not in the mock-infected cells that were adapted to hypoxia (Fig. 4A, far right). In total, these data suggest that the inhibition of translation by eIF-2α phosphorylation may limit VSV translation at early times of infection under hypoxic stress, but eIF-2α phosphorylation alone cannot explain the decrease in translational efficiency at 8 hpi and the increase in translation efficiency at 12 hpi in the hypoxia-adapted cells that are infected with VSV.

In addition to eIF-2α, the other major translation factor that is modified in VSV-infected cells is the mRNA binding eIF-4F complex. It was previously shown that VSV infection results in the dephosphorylation of cap-binding subunit eIF-4E, an event that correlates with the inhibition of host protein synthesis (12). We probed Western blots of normoxic and hypoxia-adapted cells infected with VSV by using an antibody specific for the phosphorylated form of eIF-4E (Fig. 4B). As a control for the induction of hypoxia, cell lysates were probed for the accumulation of HIF1α; actin was used as a loading control (Fig. 4C). eIF-4E was phosphorylated under mock-infected normoxic conditions and at 2 and 4 h of hypoxia adaptation and in the 8-hpi mock-infected cells that were adapted to hypoxia. There was a slight decrease in eIF-4E phosphorylation in the 12-hpi mock-infected cells that were adapted to

hypoxia, consistent with the findings of other groups (B. Wouters, personal communication). In all cases of virus-infected cells, eIF-4E was almost completely dephosphorylated. This was true of cells infected under normoxic conditions and cells infected after adaptation to hypoxia. This showed that the virus-induced changes to the eIF-4F complex were not delayed by the hypoxic stress and suggested that other changes were blocking viral translation during VSV infection of these cells.

VSV causes CPE in hypoxia. The CPE of VSV infection are characterized by cell rounding that is associated with the induction of apoptosis (25). To determine whether VSV causes CPE in hypoxic cells, HeLa cells were infected under normoxic, hypoxic, or hypoxia-adapted conditions at an MOI of 10 to insure that 100% of the cells were infected. The progress of VSV infection was monitored by phase-contrast microscopy at 8 and 12 hpi to score cells for CPE. Representative examples of these micrographs are shown in Fig. 5. Under all conditions, mock-infected cells showed no development of CPE. Cells that were infected with VSV under normoxic conditions showed rapid development of CPE, which included approximately 50% of all cells at 8 hpi and nearly 100% of all cells at 12 hpi (Fig. 5, top right). For cells in hypoxia, the results were very similar: 40 to 50% of infected hypoxic cells showed CPE by 8 hpi and 80 to 90% had rounded by 12 hpi. The hypoxia-adapted cells showed a delay at 8 hpi, but 70 to 80% of cells showed CPE by 12 hpi (Fig. 5, bottom right). When these cells were monitored for longer time periods, all cells showed CPE by 16 hpi under all conditions (data not shown). These results showed that the induction of CPE by VSV was only slightly reduced by cellular adaptation to hypoxia and that VSV retained its ability to induce CPE seen in a normoxic infection. The ability of VSV to induce CPE in hypoxic cells was observed not only in HeLa cells but also in C6 and U251 cell lines derived from glioblastomas and lung carcinoma-derived A549 cells, cancers known to develop hypoxia (32, 39) (data not shown). These results demonstrate that the ability of the virus to induce CPE under hypoxia spans multiple cancer cell types and was not cell line specific.

To determine whether VSV infection was inducing apoptosis in these cells, we probed lysates of VSV-infected HeLa cells for the presence of cleaved PARP, a protein whose cleavage is a classic hallmark of apoptosis (38). Results of this Western blot analysis can be seen in Fig. 5B. In lysates of mock-infected cells, there was no cleavage of PARP, nor was there evidence of PARP cleavage in infected cells at 8 hpi. In contrast, at 12 hpi, cleavage of PARP was visible in normoxic, hypoxic, and hypoxia-adapted cells that had been infected with VSV. This demonstrated that VSV induced both CPE and apoptosis in the hypoxic and hypoxia-adapted cells.

VSV produces progeny from hypoxic cells. The experimental results shown in Fig. 1 to 5 demonstrated that the hallmarks of VSV replication were intact in hypoxic and hypoxia-adapted cells and suggested that, in addition to infecting and killing hypoxia-adapted cancer cells, VSV may also be capable of producing functional progeny virus that would infect and kill other hypoxic cells. To address this question, HeLa cells were infected at both a high MOI (10 PFU/cell) and a low MOI (0.01 PFU/cell). At 22 hpi, the production of functional progeny virus was determined by plaque assay. Infection at high MOI results in synchronous infection of nearly all of the cells, so progeny virus reflects the yield from a single cycle of virus growth. Infection at low MOI results in the initial infection of less than 1% of the cells present, so the progeny virus produced reflects the viral yield from multiple cycles of virus growth and infection. The results, shown in Fig. 6A, show that at high MOI, VSV produces equivalent amounts of virus under normoxic, hypoxic, and hypoxia-adapted conditions. At low MOI, VSV still produced high titers of progeny in all cells, though there was a 1 log decrease of virus titer in hypoxia-adapted cells compared to normoxic infected cells. This demonstrated that in a single cycle of infection, the initial inhibition of viral protein production in hypoxia-adapted cells did not inhibit the effective yield of virus (Fig. 6A). At low MOI, the virus was slightly hindered in its ability to produce progeny virus in hypoxia-adapted cells, suggesting the delay of virus production in the initially infected cells slightly delayed viral progeny production.

VSV was able to spread through the entire population of cells under all conditions as shown by analysis of CPE in Fig. 6B. As a control, normoxic cells infected with VSV at a low MOI (0.01) showed extensive CPE (Fig. 6B, top) at 22 hpi. When hypoxic and hypoxia-adapted cells were infected at an MOI of 0.01, a similar result was seen (Fig. 6B, bottom).

VSV replication in hypoxic areas of tumor xenografts. We next investigated whether the ability of VSV to replicate in hypoxia in culture extended to invasion of hypoxic areas of an established tumor. We utilized two different types of tumors for these experiments. Tumors formed by C6 glioblastoma cells were treated intratumorally via a single injection of 1×10^7 PFU or tumors formed by Ras-transformed MEFs were treated by injection of 5×10^7 PFU of VSV in the tail vein to address whether the virus can spread to hypoxic areas of the tumor from the vasculature. Following treatment with the virus, the tumor-bearing mice were injected with EF-5 to label hypoxic areas of tissue, and 1 hour later, the tumor was excised, frozen, and sectioned. Areas of EF-5 accumulation in live hypoxic cells were labeled by using an anti-EF-5 antibody conjugated to the fluorochrome Cy3. Areas of VSV replication were detected by using a primary antibody against VSV-G and a secondary antibody conjugated to FITC. VSV replication was seen in many different areas of the tumor sections, demonstrating that the virus effectively replicated in these tumors (Fig. 7A and D). In general, three separate patterns of viral replication were seen: areas where VSV replication and hypoxic tumor regions did not overlap, areas where some overlap occurred, and areas where more extensive overlap occurred. Immunolabeling of VSV-G was specifically detected in the cytoplasmic space of these cells. This is consistent with G protein localization in cytoplasmic organelles such as the endoplasmic reticulum, Golgi, and *trans*-Golgi network as well as the cell surface. The tumors also showed many areas of strong EF-5 labeling, indicating hypoxic areas (Fig. 7B and E). Figure 7A and B show an example of VSV-G staining and EF-5 staining in the same field. The merged image shown in Fig. 7C is typical of the interaction of VSV and hypoxic tissue. A majority of viral replication is seen in tissue that does not appear hypoxic, suggesting that the virus began replication in a well-oxygenated area. There is, however, a distinct population of cells that are both hypoxic and supporting VSV replication. An example of the latter is enlarged in Fig. 7G. Cells that

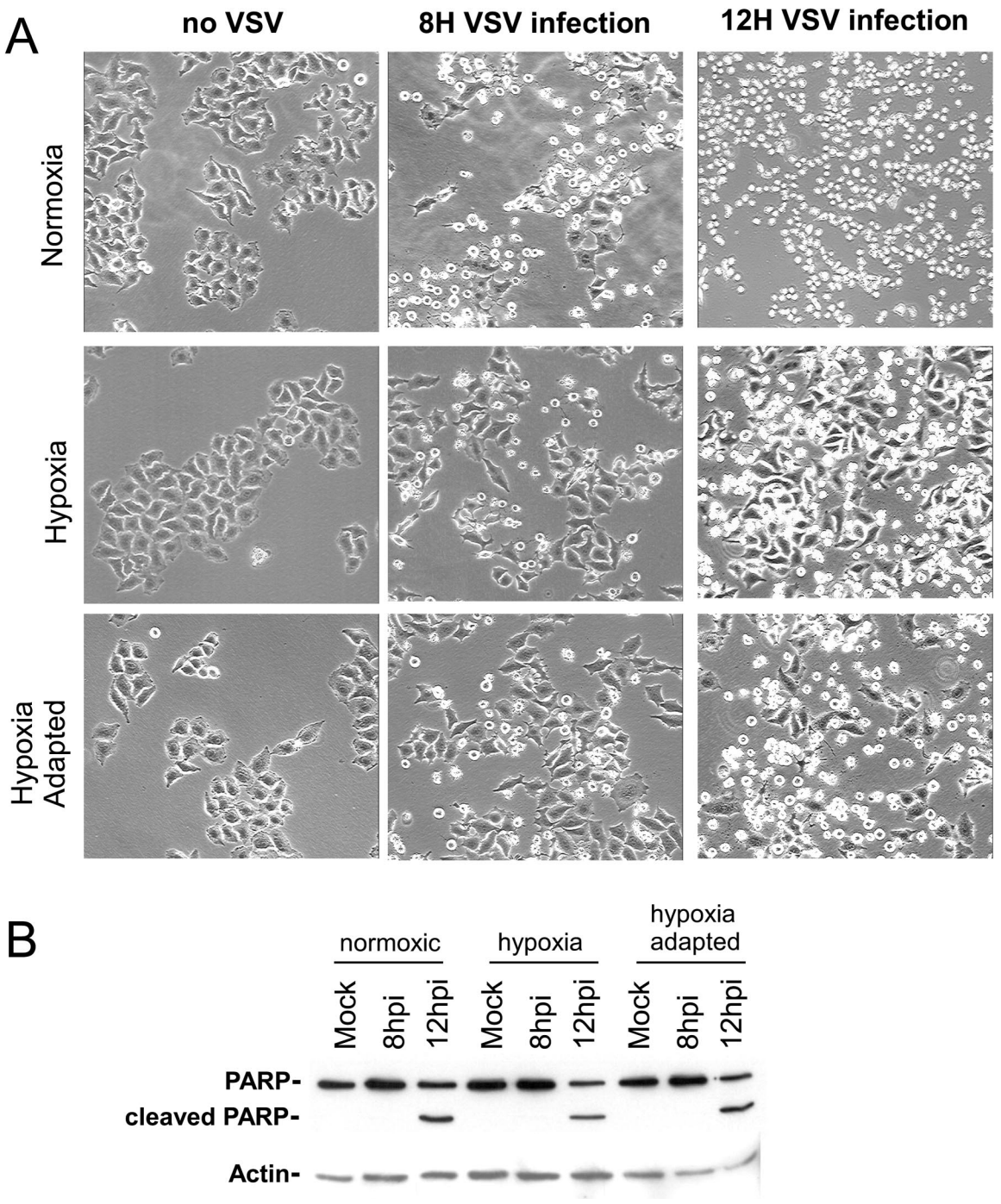

FIG. 5. (A) Images of CPE from VSV infection in normoxia and hypoxia. Cells were mock infected or infected with VSV at an MOI of 10 under normoxic, hypoxic, or hypoxia-adapted conditions, and phase-contrast images were taken at 8 and 12 hpi (8H and 12H, respectively). The phase-contrast images shown are of a representative field and are representative of the results from three separate experiments. Magnification, ×20. (B) Analysis of PARP cleavage following VSV infection. Extracts from mock- and VSV-infected cells were analyzed by Western blotting (see Materials and Methods) with antibodies to PARP and actin. Images are representative of the results from two separate experiments.

demonstrate overlap show a green-yellow cytoplasmic fluorescence and red nuclei, indicative of both viral replication and EF-5 labeling. These experiments established that VSV was capable of entering hypoxic areas of a tumor in vivo.

Similar results were obtained with tumors formed by Ras-transformed MEFs. These tumors showed evidence of viral replication (Fig. 7D) and significant areas of hypoxia (Fig. 7E). As can be seen from the combined image (Fig. 7F), VSV was indeed capable of migrating from hypoxic areas of the tumor following intravenous inoculation. Figure 7H shows an enlargement of one of the areas where viral replication and hypoxia overlapped, again showing the characteristic green cytoplasmic staining of VSV-G and red nuclear accumulation of EF-5. These results demonstrate that, in two different tumor models that develop spontaneous

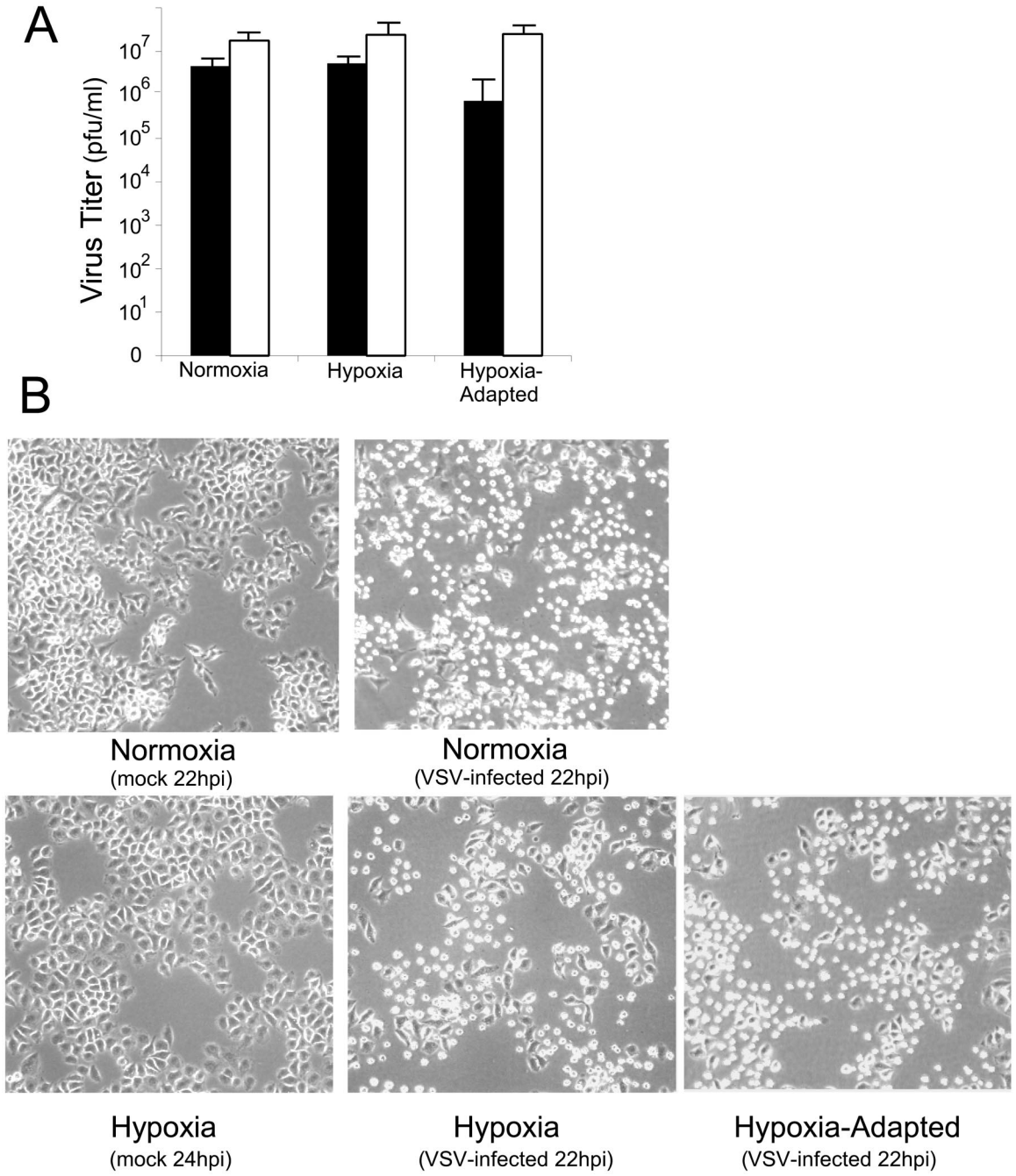

FIG. 6. VSV replication in hypoxic and hypoxia-adapted cells under single- and multiple-cycle growth conditions. (A) Virus titers determined from cells infected for 22 h at MOI of 10 (white bars) and 0.01 (black bars). Titers shown are the means (± standard deviations) of the results from three separate experiments. (B) Induction of CPE in cells infected at an MOI of 0.01. Cells were infected at an MOI of 0.01, such that ~1% of cells were initially infected, and at 22 hpi, images were taken. Images are representative of the results from three separate experiments.

hypoxic areas, VSV is capable of entering, replicating in, and traversing hypoxic areas of a tumor.

DISCUSSION

VSV has been shown to replicate preferentially in tumor cells (36). This is due to the fact that many cancer cells have defects in host antiviral response pathways, mainly the interferon pathway, which makes these cells unable to effectively combat and suppress viral replication. Normal cells, however, benefit from their intact interferon pathway and are able to suppress viral infection. This inherent difference between cancer and normal cells sets up a window of opportunity to exploit the differences in the antiviral responses of cancer tissues by utilizing viruses such as VSV, a virus that can productively infect interferon nonresponsive cells and cause apoptosis.

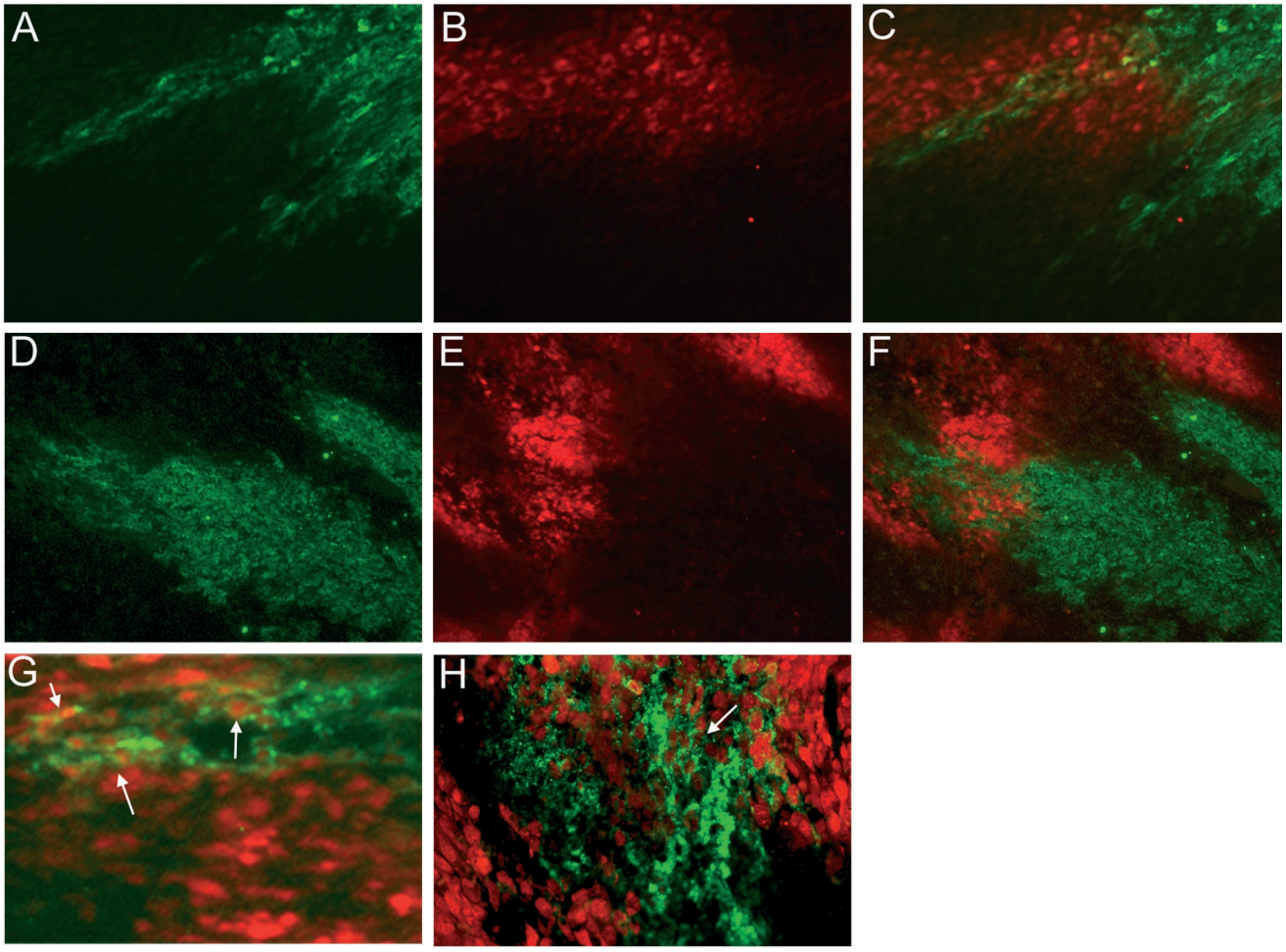

FIG. 7. VSV replication in hypoxic tumor tissue in vivo. For panels A to C and G, C6 tumors were intratumorally treated with VSV and the tumor was labeled with EF-5 in a separate injection 24 h later (see Materials and Methods). For panels D to F and H, VSV was injected intravenously into mice bearing tumors from Ras-transformed MEFs, and the tumor was labeled with EF-5 in a separate injection 36 h later. Tumors were then sectioned, and antibodies were used to detect EF-5 and VSV-G. (A and D) G protein fluorescence from a representative C6 tumor section; (B and E) EF-5 labeling in red, highlighting hypoxic areas in the same fields; (C) panel A and B images overlaid; (F) panel D and E images overlaid; (D) G protein fluorescence from a representative MEF tumor section; (G and H) higher-magnification images of C6 and MEF sections, respectively; white arrows denote areas of colocalization of hypoxia and viral replication.

Several groups have demonstrated potential advantages of using VSV as an anticancer vector, highlighting not only its ability to kill cells that are interferon nonresponsive (5, 36) but also its ability to kill cells that lack important tumor suppressors such as p53 or that are transformed by oncogenes such as Ras and Myc (6). Other studies have demonstrated that VSV is capable of causing CPE in cells that lack the executioner caspase, caspase 3 (21). Studies with syngeneic cancer models have extended these findings, demonstrating effective tumor lysis in a system with an intact immune system (14). In addition, recent work from our lab has shown that VSV can shrink existing human prostate tumors in a xenograft model (M. Ahmed and D. S. Lyles, unpublished data). All of these studies have demonstrated the potential value of VSV as an antitumor agent.

Here we have shown an additional advantage of the oncolytic virus VSV, namely its ability to replicate in a hypoxic tumor microenvironment. It is important that this replication is not a result of targeting the virus to hypoxia, and as such, this behavior is different from earlier efforts to target hypoxic areas of tumors. These previous studies have endeavored to overcome the general inhibition of cellular RNA and protein synthesis by utilizing specific elements of the cellular adaptation to hypoxia. Many have utilized DNA response elements that are activated by the hypoxia response factor HIF1α, which controls the increased transcription of a number of genes important for the hypoxic response (9, 19, 26, 30). This approach has shown some effectiveness and is clearly an important avenue to investigate. Our finding that VSV can express mRNA and translate proteins in hypoxic tissue shows that viral expression mechanisms can function effectively in this microenvironment and that VSV can replicate in hypoxic cells without specific targeting mechanisms.

The ability of VSV to replicate in vitro and in vivo under hypoxic stress is likely due to two factors: the ability of the VSV RNA polymerase to make large amounts of viral mRNA and

the ability of VSV-infected cells to translate the viral mRNA produced under hypoxic conditions. The production of large amounts of viral RNA in hypoxia-adapted cells shows that the viral RNA-dependent RNA polymerase is not sensitive to the inhibition of cellular RNA synthesis that is associated with cellular hypoxia (Fig. 2). In fact, in cells that were adapted to hypoxia, virus infection resulted in higher mRNA levels than in normoxic cells. Using VSV to express genes toxic to cancer cells, such as the herpes thymidine kinase or other suicide genes (15), may be facilitated in hypoxic tissue by this natural overproduction of mRNA in cells adapted to hypoxia.

Though VSV mRNA synthesis does not appear to be affected by the cellular response to stress, there was a clear inhibition of viral mRNA translation in hypoxia-adapted cells (Fig. 3). Though the virus appeared to overcome the cellular inhibition of protein synthesis, it never appeared to reach the level seen in a normoxic infection. Infection of all cells, however, resulted in the dephosphorylation of eIF-4E and the almost complete inhibition of host protein synthesis. This inhibition of host translation may be an additional advantage of using the virus to attack hypoxic cells, as it can block the cell's ability to produce proteins important for maintaining the adaptation to hypoxia.

The altered timing of both viral mRNA accumulation and translation in hypoxia-adapted cells demonstrates the inherent capacity of VSV to adapt to this cellular stress. The ability to overproduce mRNA and to overcome the initial inhibition of translation (Fig. 3) may be a response to the presence of eIF-2α phosphorylation (Fig. 4A) acting as an inhibitor of viral translation in hypoxia-adapted cells. It is not immediately apparent why there is less eIF-2α phosphorylation at 12 hpi in the hypoxia-adapted cells infected with VSV versus the normoxic infected cells. It is possible, however, that the hypoxia-adapted cells have begun to express GADD-34, a protein that increases eIF-2α phosphatase activity. GADD-34 is induced by hypoxic stress (C. Koumenis, unpublished data), and thus, in the hypoxia-adapted cells, this protein may act to reduce the level of eIF-2α phosphorylation during the subsequent VSV infection.

The mechanism VSV utilizes to overcome the initial inhibition of viral translation in cells undergoing hypoxic stress does not appear to be solely related to eIF-2α phosphorylation. eIF-2α phosphorylation persists throughout VSV infection, yet VSV messages are more efficiently translated at later times of infection. Recent reports have suggested that translation inhibition by eIF-2α in transformed cells is defective (4, 29). It is possible that VSV translation is inhibited by other effects of hypoxia on translation initiation or even elongation, but this will require further study.

The ability of VSV to replicate and cause CPE and apoptosis in hypoxia (Fig. 5) is important for VSV's potential as an oncolytic agent. To successfully treat any tumor, a therapeutic agent would ideally display the ability to overcome different microenvironments found in a tumor mass. Our studies show that in vitro, even when only 1% of cells are initially infected in an anoxic environment, VSV spreads through and causes CPE of the entire population, highlighting the virus's ability to adapt and replicate under this severe oxygen depletion. Further, our results from the implanted tumors showed that VSV not only replicated in regions of tumor hypoxia it was also able to spread to those regions following blood-borne delivery and was able to propagate through these regions. VSV's ability to arrive at a treatment site by a vascular avenue and its ability to infect and spread to and through regions of low-oxygen tension is critical. This behavior should allow VSV to infect and kill cells within an otherwise unfavorable tumor environment.

VSV's ability to replicate in hypoxia raises several additional questions. One is whether this property is unique to VSV or whether other oncolytic viruses such as adenovirus, Newcastle disease virus, or reovirus share the same ability to replicate under low-oxygen conditions. Based on work with simian virus 40 showing that hypoxia blocks viral DNA replication (33, 34), we believe that DNA viruses will face additional challenges to successful replication in hypoxia because of the inhibition of DNA synthesis. In contrast, RNA viruses like VSV, Newcastle disease virus, and reovirus may, as a class, be capable of surmounting the cellular adaptation to hypoxia to infect and kill cells. In addition, there may also be the possibility of controlling VSV or a related virus through specific RNA elements so that its replication is specifically restricted to hypoxic conditions.

ACKNOWLEDGMENTS

We thank Griffith Parks, Maryam Ahmed, Laurant Poliquin, and Rebecca Connor for helpful advice and manuscript comments. Thanks also to the Cancer Center Analytical Imaging Facility (supported by CA 12197 to the Comprehensive Cancer Center of Wake Forest University) for phosphorimaging resources.

This work was supported by Public Health Service grants RO1AI32983 and RO1AI 052304 from NIAID and DOD Prostate Cancer Research Program grant DAMD17-02-1-0155 to D.S.L. and grant RO1CA94214 to C.K. J.H.C. was supported by Signal Transduction Mechanisms and Cell Function training program grant T32CA-09422 from NCI and Public Health Service grant F32AI051805 from NIAID.

REFERENCES

1. **Ahmed, M., M. O. McKenzie, S. Puckett, M. Hojnacki, L. Poliquin, and D. S. Lyles.** 2003. Ability of the matrix protein of vesicular stomatitis virus to suppress beta interferon gene expression is genetically correlated with the inhibition of host RNA and protein synthesis. J. Virol. **77:**4646–4657.
2. **Andreansky, S. S., B. He, G. Y. Gillespie, L. Soroceanu, J. Markert, J. Chou, B. Roizman, and R. J. Whitley.** 1996. The application of genetically engineered herpes simplex viruses to the treatment of experimental brain tumors. Proc. Natl. Acad. Sci. USA **93:**11313–11318.
3. **Arsham, A. M., J. J. Howell, and M. C. Simon.** 2003. A novel hypoxia-inducible factor-independent hypoxic response regulating mammalian target of rapamycin and its targets. J. Biol. Chem. **278:**29655–29660.
4. **Balachandran, S., and G. N. Barber.** 2004. Defective translational control facilitates vesicular stomatitis virus oncolysis. Cancer Cell **5:**51–65.
5. **Balachandran, S., and G. N. Barber.** 2000. Vesicular stomatitis virus (VSV) therapy of tumors. IUBMB Life **50:**135–138.
6. **Balachandran, S., M. Porosnicu, and G. N. Barber.** 2001. Oncolytic activity of vesicular stomatitis virus is effective against tumors exhibiting aberrant p53, Ras, or myc function and involves the induction of apoptosis. J. Virol. **75:**3474–3479.
7. **Bell, J. C., B. Lichty, and D. Stojdl.** 2003. Getting oncolytic virus therapies off the ground. Cancer Cell **4:**7–11.
8. **Bergmann, M., I. Romirer, M. Sachet, R. Fleischhacker, A. Garcia-Sastre, P. Palese, K. Wolff, H. Pehamberger, R. Jakesz, and T. Muster.** 2001. A genetically engineered influenza A virus with ras-dependent oncolytic properties. Cancer Res. **61:**8188–8193.
9. **Binley, K., Z. Askham, L. Martin, H. Spearman, D. Day, S. Kingsman, and S. Naylor.** 2003. Hypoxia-mediated tumour targeting. Gene Ther. **10:**540–549.
10. **Brahimi-Horn, C., E. Berra, and J. Pouyssegur.** 2001. Hypoxia: the tumor's gateway to progression along the angiogenic pathway. Trends Cell Biol. **11:**S32–S36.
11. **Brown, J. M.** 2002. Tumor microenvironment and the response to anticancer therapy. Cancer Biol. Ther. **1:**453–458.
12. **Connor, J. H., and D. S. Lyles.** 2002. Vesicular stomatitis virus infection alters the eIF4F translation initiation complex and causes dephosphorylation of the eIF4E binding protein 4E-BP1. J. Virol. **76:**10177–10187.

13. **Dubensky, T. W., Jr.** 2002. (Re-)Engineering tumor cell-selective replicating adenoviruses: a step in the right direction toward systemic therapy for metastatic disease. Cancer Cell **1:**307–309.
14. **Ebert, O., K. Shinozaki, T. G. Huang, M. J. Savontaus, A. Garcia-Sastre, and S. L. Woo.** 2003. Oncolytic vesicular stomatitis virus for treatment of orthotopic hepatocellular carcinoma in immune-competent rats. Cancer Res. **63:**3605–3611.
15. **Fernandez, M., M. Porosnicu, D. Markovic, and G. N. Barber.** 2002. Genetically engineered vesicular stomatitis virus in gene therapy: application for treatment of malignant disease. J. Virol. **76:**895–904.
16. **Graeber, T. G., C. Osmanian, T. Jacks, D. E. Housman, C. J. Koch, S. W. Lowe, and A. J. Giaccia.** 1996. Hypoxia-mediated selection of cells with diminished apoptotic potential in solid tumours. Nature **379:**88–91.
17. **Harris, A. L.** 2002. Hypoxia–a key regulatory factor in tumour growth. Nat. Rev. Cancer **2:**38–47.
18. **Hawkins, L. K., N. R. Lemoine, and D. Kirn.** 2002. Oncolytic biotherapy: a novel therapeutic platform. Lancet Oncol. **3:**17–26.
19. **Hernandez-Alcoceba, R., M. Pihalja, D. Qian, and M. F. Clarke.** 2002. New oncolytic adenoviruses with hypoxia- and estrogen receptor-regulated replication. Hum. Gene Ther. **13:**1737–1750.
20. **Hirasawa, K., S. G. Nishikawa, K. L. Norman, M. C. Coffey, B. G. Thompson, C. S. Yoon, D. M. Waisman, and P. W. Lee.** 2003. Systemic reovirus therapy of metastatic cancer in immune-competent mice. Cancer Res. **63:** 348–353.
21. **Hobbs, J. A., G. Hommel-Berrey, and Z. Brahmi.** 2003. Requirement of caspase-3 for efficient apoptosis induction and caspase-7 activation but not viral replication or cell rounding in cells infected with vesicular stomatitis virus. Hum. Immunol. **64:**82–92.
22. **Hochachka, P. W., L. T. Buck, C. J. Doll, and S. C. Land.** 1996. Unifying theory of hypoxia tolerance: molecular/metabolic defense and rescue mechanisms for surviving oxygen lack. Proc. Natl. Acad. Sci. USA **93:**9493–9498.
23. **Hockel, M., K. Schlenger, B. Aral, M. Mitze, U. Schaffer, and P. Vaupel.** 1996. Association between tumor hypoxia and malignant progression in advanced cancer of the uterine cervix. Cancer Res. **56:**4509–4515.
24. **Huang, T. G., O. Ebert, K. Shinozaki, A. Garcia-Sastre, and S. L. Woo.** 2003. Oncolysis of hepatic metastasis of colorectal cancer by recombinant vesicular stomatitis virus in immune-competent mice. Mol. Ther. **8:**434–440.
25. **Kopecky, S. A., and D. S. Lyles.** 2003. The cell-rounding activity of the vesicular stomatitis virus matrix protein is due to the induction of cell death. J. Virol. **77:**5524–5528.
26. **Koshikawa, N., K. Takenaga, M. Tagawa, and S. Sakiyama.** 2000. Therapeutic efficacy of the suicide gene driven by the promoter of vascular endothelial growth factor gene against hypoxic tumor cells. Cancer Res. **60:**2936–2941.
27. **Koumenis, C., C. Naczki, M. Koritzinsky, S. Rastani, A. Diehl, N. Sonenberg, A. Koromilas, and B. G. Wouters.** 2002. Regulation of protein synthesis by hypoxia via activation of the endoplasmic reticulum kinase PERK and phosphorylation of the translation initiation factor eIF2α. Mol. Cell. Biol. **22:**7405–7416.
28. **Obuchi, M., M. Fernandez, and G. N. Barber.** 2003. Development of recombinant vesicular stomatitis viruses that exploit defects in host defense to augment specific oncolytic activity. J. Virol. **77:**8843–8856.
29. **Perkins, D. J., and G. N. Barber.** 2004. Defects in translational regulation mediated by the alpha subunit of eukaryotic initiation factor 2 inhibit antiviral activity and facilitate the malignant transformation of human fibroblasts. Mol. Cell. Biol. **24:**2025–2040.
30. **Post, D. E., and E. G. Van Meir.** 2003. A novel hypoxia-inducible factor (HIF) activated oncolytic adenovirus for cancer therapy. Oncogene **22:**2065–2072.
31. **Probst, G., H. J. Riedinger, P. Martin, M. Engelcke, and H. Probst.** 1999. Fast control of DNA replication in response to hypoxia and to inhibited protein synthesis in CCRF-CEM and HeLa cells. Biol. Chem. **380:**1371–1382.
32. **Rampling, R., G. Cruickshank, A. D. Lewis, S. A. Fitzsimmons, and P. Workman.** 1994. Direct measurement of pO2 distribution and bioreductive enzymes in human malignant brain tumors. Int. J. Radiat. Oncol. Biol. Phys. **29:**427–431.
33. **Riedinger, H. J., M. van Betteraey, and H. Probst.** 1999. Hypoxia blocks in vivo initiation of simian virus 40 replication at a stage preceding origin unwinding. J. Virol. **73:**2243–2252.
34. **Riedinger, H. J., M. van Betteraey-Nikoleit, U. Hilfrich, K. H. Eisele, and H. Probst.** 2001. Oxygen-dependent regulation of in vivo replication of simian virus 40 DNA is modulated by glucose. J. Biol. Chem. **276:**47122–47130.
35. **Sinkovics, J. G., and J. C. Horvath.** 2000. Newcastle disease virus (NDV): brief history of its oncolytic strains. J. Clin. Virol. **16:**1–15.
36. **Stojdl, D. F., B. Lichty, S. Knowles, R. Marius, H. Atkins, N. Sonenberg, and J. C. Bell.** 2000. Exploiting tumor-specific defects in the interferon pathway with a previously unknown oncolytic virus. Nat. Med. **6:**821–825.
37. **Stojdl, D. F., B. D. Lichty, B. R. Tenoever, J. M. Paterson, A. T. Power, S. Knowles, R. Marius, J. Reynard, L. Poliquin, H. Atkins, E. G. Brown, R. K. Durbin, J. E. Durbin, J. Hiscott, and J. C. Bell.** 2003. VSV strains with defects in their ability to shutdown innate immunity are potent systemic anti-cancer agents. Cancer Cell **4:**263–275.
38. **Tewari, M., L. T. Quan, K. O'Rourke, S. Desnoyers, Z. Zeng, D. R. Beidler, G. G. Poirier, G. S. Salvesen, and V. M. Dixit.** 1995. Yama/CPP32 beta, a mammalian homolog of CED-3, is a CrmA-inhibitable protease that cleaves the death substrate poly(ADP-ribose) polymerase. Cell **81:**801–809.
39. **Volm, M., and R. Koomagi.** 2000. Hypoxia-inducible factor (HIF-1) and its relationship to apoptosis and proliferation in lung cancer. Anticancer Res. **20:**1527–1533.